SciMedCentral

JSM Nanotechnology & Nanomedicine

Research Article

Doxorubicin-Conjugated Bisphosphonate Nanoparticles for the Therapy of Osteosarcoma

Rudnick-Glick S, Corem-Salkmon E, Grinberg I, Gluz E and Margel S*

Department of Chemistry, Bar-Ilan University, Israel

Corresponding author

Shlomo Margel, The Institute of Nanotechnology and Advanced Materials, Department of Chemistry, Bar-Ilan University, Ramat-Gan 52900, Israel, Tel: +972-3-5318861; Email: shlomo.margel@mail.biu.ac.il

Submitted: 24 June 2014

Accepted: 19 July 2014

Published: 21 July 2014

Keywords

- Bisphosphonate nanoparticles
- Osteosarcoma
- Doxorubicin
- Targeted drug delivery

Abstract

Osteosarcoma is amongst the most common primary malignant tumors of bone and occurs in adolescents and young adults. Current treatment is a combination of both surgery and chemotherapeutics. However, the use of anticancer drugs is still associated with serious side effects. In this article we describe a doxorubicin drug delivery system based on bisphosphonate nanoparticles with a narrow size distribution. We have shown that the doxorubicin-conjugated bisphosphonate nanoparticles preferentially target the bone tumor, thereby increasing the anti-cancer drug bioavailability to the tumor. Furthermore, we have been able to demonstrate that the doxorubicin-conjugated bisphosphonate nanoparticles have significantly higher activity than the free drug both in vitro and in vivo. Testing the doxorubicin-conjugated bisphosphonate nanoparticles on an osteosarcoma xynograph in a chicken embryo model demonstrated that these nanoparticles specifically targeted the tumor and thus decreased the tumor size.

ABBREVIATIONS

BP: Bisphosphonates; HAP: Hydroxyapatite; NPs: Nanoparticles; MA-PEG-BP: Methacrylate PEG Bisphosphonate; APMA: N-(3-aminopropyl) Methacrylamide Hydrochloride; PEG: Polyethylene Glycol; MA-PEG: Polyethylene Glycol Methacrylate; TTEGDA: Tetraethylene Glycol Dimethacrylate; MA-PEG-OCH3: Methacrylate ether; PPS: Potassium Persulfate; PEG-NHS: O-[(N-Succinimidyl)succinyl-aminoethyl-O'-methylpolyethylene glycol; HCl: Hydrochloric Acid; DMF: Anhydrous N,N-dimethylformamide; NHS-PEG-NHS: O,O'-Bis [2-(N- Succinimidyl-succinylamino)ethyl]polyethylene Glycol; APMA: N-(3-aminopropyl) methacrylamide hydrochloride; PBS: Dulbecco's Phosphate-Buffered Saline; DMEM: Dulbecco's minimum essential medium; NIR: Near IR; ξ potential: Zeta potential; E**:** Embryonic day; CAM: Chorioallantoic Membrane; doxo: Doxorubicin; IV: Intravenous.

INTRODUCTION

Osteosarcoma (OS) is amongst the most common primary malignant tumors of bone occurring in both adolescents and young adults [1,2]. Current treatment is a combination of both surgery and chemotherapeutics. Combinations of high doses of doxorubicin [3] methotrexate [4,5], cisplatin and ifosfamide [6] have led to a significant improvement in survival rate. However, the use of anticancer drugs is still associated with serious side effects, due to nonspecific uptake and in the case of OS a poor bone blood supply [7] necessitating the use of toxic high dosages. In addition, drug-resistant phenotypes and "secondary malignancies" [8] occur. Therefore, the development of bone-targeted anti- tumor agents with minimal or no side effects for the prevention and treatment of cancer- associated bone diseases remains a priority [9].

Bisphosphonates (BP) are the primary drug used for the treatment of bone diseases such as osteoporosis, Paget's disease, benign and malignant bone diseases, etc. [10-14]. BP are a chemical analog to endogenous pyrophosphate, have a High Affinity to Hydroxyapatite (HAP) and exhibit potent bone resorption inhibitory activity [15,16], due to their similarity to pyrophosphate. Whereas in pyrophosphate the oxygen atom binds to two phosphorus atoms (P–O–P) in BP the oxygen is substituted by a carbon atom (P–C–P), thus increasing BP resistance to chemical and enzymatic degradation [16,17]. Due to BP compounds high affinity to Ca^{+2} ions they can used for bone targeting in areas with high resorption activity [18,19].

Submicron-sized polymeric particles (3-200 nm) [20] have aroused considerable interest in the area of drug delivery [21,22]. Many scientific groups have focused their efforts to improve Nanoparticles (NPs) targeting to recipient cells and tissues [23-27]. In addition, due to NPs submicron size they are

able to bypass the body's drug resistance mechanism and thus increase the intracellular drug concentration in cancer cells while avoiding toxicity of normal cells [28-30].

A novel BP NPs has been recently synthesized in our laboratory [31-34]. The BP NPs are constructed of three monomers: Methacrylate PEG Bisphosphonate (MA-PEG-BP) monomer, a monomer containing a primary amine group (N-(3-aminopropyl) methacrylamide hydrochloride, APMA) and a crosslinker monomer to form a crosslinked particle. The novel BP NPs possess high concentration of PEG in order to increase the half-life time of the NPs in the blood [35] as well as a dual functionality: chelation to the bone mineral - HAP, through the BP group, and covalent attachment to carboxylate (or carboxylate derivatives) compounds via the primary amine groups. These BP NPs have shown insignificant toxicity and high affinity to bone, and therefore suggest that they can be a good candidate for drug delivery to bone tumors [31,34].

In this article we describe the drug delivery and therapeutic ability of doxorubicin- conjugated BP NPs. Doxorubicin was conjugated covalently to the primary amine group on the BP NPs through a PEG spacer. The doxorubicin-conjugated BP NPs have shown high toxicity to osteosarcoma cells, as well as high affinity to osteosarcoma tumors in a chicken embryo model.

EXPERIMENTAL PART

Materials

The following analytical-grade chemicals were purchased from commercial sources and used without further purification: polyethylene glycol methacrylate (MA-PEG, Mn 360), Tetraethylene Glycol Dimethacrylate (TTEGDA), polyethylene glycol methacrylate ether (MA-PEG-OCH3, Mn 300), Potassium Persulfate (PPS), O-[(N-Succinimidyl) succinyl-aminoethyl-O'-methylpolyethylene glycol (PEG-NHS, Mw 750), polyvinylpyrrolidone (PVP, Mw 360K), sodium hydroxide (NaOH, 1 N), hydrochloric acid (HCl, 1 N), anhydrous dichloromethane, anhydrous N,N-Dimethylformamide (DMF), chromium oxide, isopropanol, magnesium sulfate (97%), triethylamine (99%), methanesulfonyl chloride, sodium chloride, sodium azide (99.5%), triphenylphosphine, glycine and O,O'- Bis[2-(N-Succinimidyl-succinylamino)ethyl]polyethylene glycol (NHS-PEG-NHS ,MW 3,000) from Sigma (Rehovot, Israel); N-(3-aminopropyl) methacrylamide hydrochloride, (APMA) from Polysciences, Inc. (Warrington, PA) Dialysis membrane (1000 K-16MM), bicarbonate buffer (BB, 0.1 M, pH 8.4), sodium carbonate and sodium bicarbonate from Bio-Lab Ltd. (Jerusalem, Israel); Cy 3-NHS ester and Cy 7-NHS ester from Lumiprobe Corporation (Florida, USA); Doxorubicin hydrochloride from wonda science (Massachusetts, USA). Dulbecco's phosphate-buffered saline (PBS), Dulbecco's Minimum Essential Medium (DMEM) , fetal bovine serum, glutamine, penicillin and streptomycin from Biological Industries (Bet Haemek, Israel); Human cell lines Saos-2 and U-2OS from the American Type Culture Collection (Manassus, VA); Marigel from Sigma (Germany); Water was purified by passing deionized water through an Elgastat Spectrum reverse osmosis system (Elga Ltd., High Wycombe, UK).

Synthesis of the BP NPs

BP NPs were prepared similarly to that described in the literature [31,32]. Briefly, 45 mg MA-PEG-BP, 5 mg APMA and 50 mg TTEGDA (total monomers concentration was 5 % w/v) were added to a vial containing 8 mg of PPS (8 % w/w) as initiator and 20 mg PVP 360K (1 % w/v) as stabilizer dissolved in 2 mL of BB. For the polymerization, the vial containing the mixture was purged with N2 to exclude air and then shaken at 83°C for 8h. The obtained BP nanoparticles were washed of excess reagents by extensive dialysis cycles (cut-off of 1000 k) with purified water.

Synthesis of the NIR fluorescent BP NPs

Near IR (NIR) fluorescent BP NPs were synthesized similarly to describe in the literature [32]. In brief, NIR fluorescent BP NPs were prepared by reaction of the primary amino groups on the BP NPs with Cy7-NHS ester. Cy7-NHS ester (2 mg) was dissolved in 0.5 mL of anhydrous DMSO. 250 μL of the Cy7-NHS ester solution was then added to 5 mL of the BP NPs dispersion in BB (2 mg/mL), and the reaction was stirred overnight at rt. Blocking of residual amine groups was then accomplished by adding 0.5 mg of PEG-NHS to the obtained NIR fluorescent BP nanoparticles aqueous dispersion. The reaction was then stirred 30 min at rt. The obtained NIR fluorescent-conjugated BP nanoparticles were then washed from excess reagents by extensive dialysis in water. Cy3- NHS ester was conjugated to the BP NPs in a similar manner.

NIR fluorescent control nanoparticles possessing OCH3 groups instead of the BP groups, for the chicken embryo body distribution experiments, were prepared similarly substituting the monomer MA-PEG-BP for MA-PEG-OCH3.

Synthesis of the doxorubicin-conjugated BP NPs

Doxorubicin-conjugated BP NPs were prepared by an initial reaction of the primary amine group on the BP NPs with NHS-PEG-NHS followed by the addition of doxorubicin. Briefly, NHS-PEG-NHS (10 mg) was dissolved in Double Distilled Water (DDW) (1 mL). 500 μL of the NHS-PEG-NHS solution was then added to 5 mL of the BP NPs dispersion in BB (2 mg/mL), and the reaction was stirred at rt. After 10 min, 1 mg doxorubicin, which initially dissolved in DDW, was added to the dispersion and was stirred for an additional 1 h. Blocking of residual amine groups was then accomplished by adding 50 mg of glycine to the doxorubicin BP NPs aqueous dispersion. The reaction was then stirred for a further 30 min at rt. The obtained doxorubicin-conjugated BP NPs were then washed from excess reagents by extensive dialysis in water. The concentration of the conjugated doxorubicin was determined using fluorescent intensity (3ex 470 nm; 3em 590 nm).

Extent of doxorubicin leakage

Leakage of doxorubicin conjugated to the BP NPs into the continuous phase (PBS containing 4% HSA) was evaluated according to the following procedure: doxorubicin- conjugated BP NPs dispersed in PBS (1 mg/mL) containing 4% HSA were shaken at 37°C for 12 h and then filtered via a 300 kDa filtration tube (VS0241 Viva Spin) at 4000 rpm (Centrifuge CN-2200 MRC). The fluorescence intensity of the supernatant was then measured at 3ex=470 nm; 3em=590 nm.

Characterization of the BP nanoparticles

Dried particle size and size distribution were measured with

Transmission Electron Microscopy (TEM). TEM images were obtained with a FEI TECNAI C2 BIOTWIN electron microscope with 120 kV accelerating voltage. Samples for TEM were prepared by placing a drop of diluted sample on a 400-mesh O2 plazma etched carbon-coated copper grid. The average particle size and size distribution were determined by the measurement of the diameter of approximately 200 particles. Hydrodynamic diameter and size distribution of the particles dispersed in double distilled water were measured at rt with a particle analyzer–model NANOPHOX (Sympatec GmbH, Germany). Electro- kinetic properties (ξ potential) of the formed particles were measured using a titration method, from pH 2 to 11 with HCl 0.1 M and NaOH 0.1 M. The measurements were made at a constant NPs concentration of 0.1 mg/ml. The ξ potential of the formed particles were measured by ξ potential analyzer model Zeta Potential WALLIS (Cordouan Technologies, France).

Cell lines of human Saos-2 and U-2OS colorectal adenocarcinoma cell lines were used for the following experiments. The cell lines were maintained in DMEM supplemented with heat-inactivated fetal bovine serum 10%, penicillin 100 IU/mL, streptomycin 100 3g/mL, and l-glutamine 2 mM. Cell lines were screened using a mycoplasma detection kit to ensure that they remained mycoplasma-free [36].

Cell viability test (XTT)

In vitro toxicity of the doxorubicin-conjugated BP NPS was tested using two types of cancer cell lines, human osteosarcoma Saos-2 and U-2OS [37-39]. XTT assay was used in order to assess cell viability. The doxorubicin- conjugated BP NPs were freshly dispersed in PBS and then added to the 95% confluent cell culture in culture medium so that the final concentration of conjugated doxorubicin BP NPs was 8 and 40 μg/mL giving a final concentration of doxorubicin of 50 and 250 ng/ml respectively. The cell cultures were further incubated at 37°C in a humidified 5% CO2 incubator and then checked for cellular toxicity after 48 and 72 h. The percentage of cell cytotoxicity was calculated as shown in the manufacturer's protocol of the XTT toxicity detection kit. All samples were tested in six folds.

BP NPs targeting and therapeutic activity in a chicken embryo model seeded with Saos-2 cells

Experiments were performed according to the protocols of the Israeli National Council for Animal Experiments. Fertile chicken eggs obtained from a commercial supplier were incubated at 37°C at 60–70% humidity in a forced-draft incubator, as described in the literature [36,40]. On embryonic day (E) E8 of incubation, a window was opened in the shell, and the chorioallantoic membrane (CAM) was exposed. A total of $6x10^5$ Saos2 cells were mixed in 30 μl of Matrigel and then implanted on a plastic ring placed on the CAM. On E13, a total of 100 μL of 0.1 mg/mL of the Cy7-conjugated cross linked BP NPs dispersed in PBS and of the control fluorescent NPs (wherein the BP groups were substituted by OCH3 groups) dispersed in PBS were Injected Intravenously (IV) into a large CAM blood vessel. After injection, the window in the egg's shell was sealed with cellotape, and the chicken embryos were returned to incubation for different time periods of 4, 24 48 and 72 h. Each experiment group contained 7 embryos. The fluorescence intensity of the NIR fluorescent BP and control NPs was studied by the Maestro II *in vivo* imaging system, 2D planar fluorescence imaging of small animals (Cambridge Research & Instrumentation, Inc., Woburn, MA). A NIR excitation/emission filter set was used for our experiments (3ex: 710–760 nm, 3em > 750 nm). The Liquid Crystal Tunable Filter (LCTF) was programmed to acquire image cubes from 3 = 790 nm to 860 nm with an increment of 10 nm per image. Fluorescence intensity measurements were performed using ImageJ software [41]. The tumor samples were transferred onto black paper and then imaged.

In a similar manner, doxorubicin-conjugated BP NPs (0.1 mg/ml containing 0.5 μg conjugated doxorubicin) and free doxorubicin (10 μg/ml) were injected on E12. The tumor was extracted after 96 h and weighed. All the experiment with chicken embryos were repeated twice with similar results.

To decrease animal suffer, the experiment with chicken embryos were terminated after E16.

RESULTS AND DISCUSSION

Synthesis and characterization of the doxorubicin-conjugated BP NPs

Doxorubicin-conjugated BP NPs for osteosarcoma therapy were prepared according to Figure 1, as described in the experimental section. The measured dry diameter of the BP NPs was 52.3 ± 21 nm. The doxorubicin was then covalently conjugated to the BP NPs, via a PEG spacer, through the free amine groups on the surface of the BP NPs. Due to the conjugation the dry diameter of these NPs increased slightly from 52.3 ± 21 nm to 62.7 ± 21 nm (Figure 2A). An inverse behavior was observed for the hydrodynamic diameters, as shown in Figure 2B, e.g., the hydrodynamic diameter decreased from 160 ± 17 nm for the BP NPs to 155 ± 20 nm for the doxorubicin-conjugated BP NPs. The slight decrease in the hydrodynamic diameter could be attributed to the increased surface hydrophobicity as a result of the doxorubicin binding. The leakage of doxorubicin from the BP NPs to PBS containing 4% HSA was investigated according to the description in the experimental section. After 12 h incubation at 37°C no detected leakage was observed.

The concentration of the doxorubicin conjugated to the BP NPs was determined by measuring the fluorescence of the bound drug ((3ex 470; (3em 590) as described in the experimental section. Investigation of the binding of doxorubicin to the BP NPs (10 mg) using different concentrations of doxorubicin (0.2, 1 and 2 mg) and of NHS-PEG-NHS (0.2, 1, and 5 mg) was evaluated. It was found that in all combinations 5 μg of doxorubicin was conjugated to 1 mg of the BP NPs. Hence we can conclude that the concentrations which we used for the binding were in excess. The doxorubicin binding yields for the different concentrations of doxorubicin (0.2, 1 and 2 mg), with a constant concentration of NHS-PEH-NHS (5 mg) were calculated to be 3, 5 and 30 %, respectively. Increasing the concentration of NHS-PEG-NHS (0.2, 1, and 5 mg) while using a constant concentration of doxorubicin (1 mg), did not affect the concentration of the bound doxorubicin. It should be noted that in the continuation of the present study we used 5 μg conjugated doxorubicin for each mg of the BPs NPs as described above.

The change in the charge of the doxorubicin-conjugated BP NPs as a function of pH was evaluated using zeta (ξ) potential

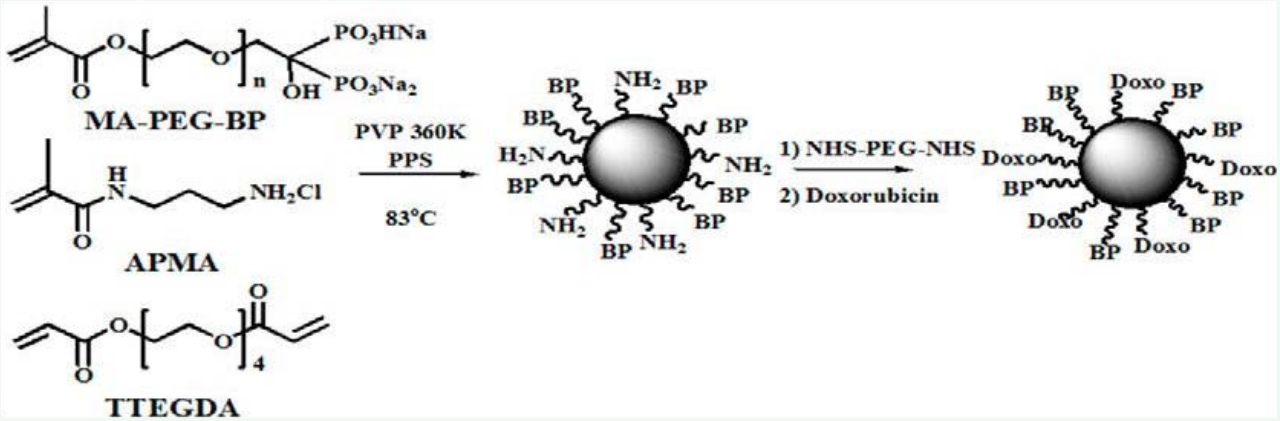

Figure 1 Scheme of the synthesis of the doxorubicin-conjugated BP NPs.

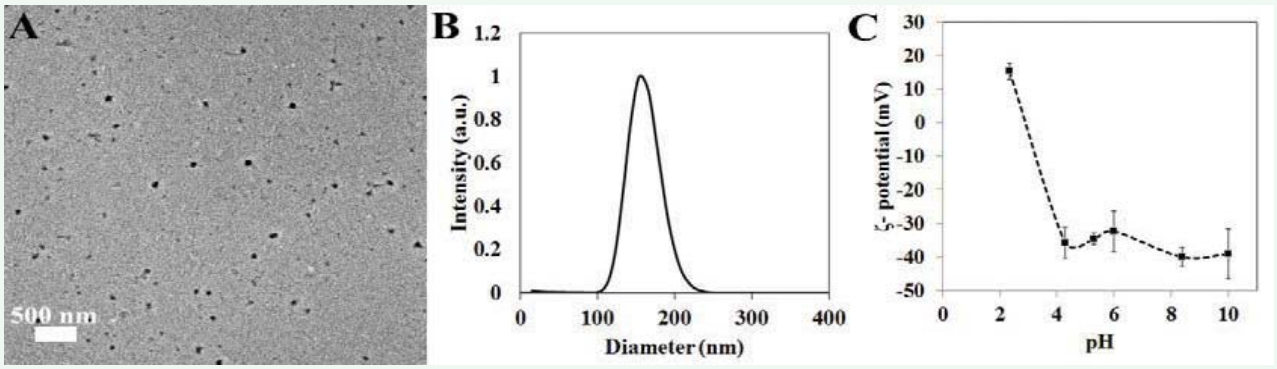

Figure 2 TEM image (A), size histogram (B) and ξ-potential (C) of the doxorubicin- conjugated BP NPs (Error bars represent standard deviation).

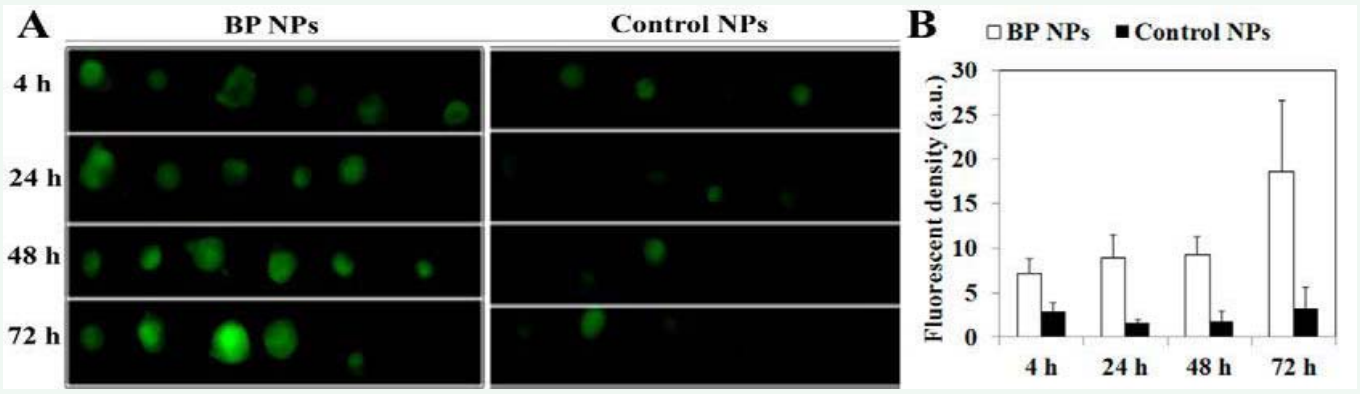

Figure 3 A photomicrograph (A) and histogram (B) showing the kinetics of the tumor marking by the NIR fluorescent BP and the control NPs in a chicken embryo model. On E8 of incubation, a total of 6x105 Saos-2 cells were implanted in a plastic ring placed on the CAM. On E13, a total of 100 µL of 0.1 mg/mL of the Cy7-conjugated BP NPs or the Cy7-conjugated control NPs dispersed in PBS were IV injected into a large CAM blood vessel. The chicken embryos were then returned to incubation for different time periods (4, 24 48 and 72 h).

(Figure 2C). Doxorubicin-conjugated BP NPs, exhibit a decrease in the ξ-potential as the pH increases up to about 5.0, then up to about pH 10.0 the ξ-potential did not significantly affected by the increase in the pH. Around physiological pH (pH 7.4) the ξ-potential is found to be -40 mV, as seen in Figure 2C. The pI of doxorubicin-conjugated BP NPs as shown in Figure 2C was measured to be 2.9 mV. These finding support that the doxorubicin-conjugated BP NPs maintain their stability in physiological pH.

Tumor targeting and therapeutic activity of the BP NPs

Privious *in vivo* testing on a chicken embryo model, by our group, demonstrated a high affinity of the NIR fluorescent BP NPs to bones as opposed to other organs [31]. In the present study

we examined the BP NPs ability to target osteosarcoma tumor in a CAM model, by initially implanting Saos-2 cells on the CAM of a chicken embryo, as described in the experimental section [32]. Saos-2 cell were chosen due to their ability to form solid tumors, as opposed to U-2OS cells that did not form a prominent solid tumor in the CAM model. The NIR fluorescent BP NPs and the NIR fluorescent control NPs (similar particles except the BP groups were replaced with methoxy groups, as described in the experimental section) were IV injected to the chicken embryo and the kinetics of the fluorescence in the blood and tumor were followed for 4, 24, 48 and 72 h. 48 h after the IV injection both the Cy7-conjugated BP NPs and the Cy7-conjugated control NPs could not be detected in the blood. In contrast, the fluorescence intensity of the Saos-2 tumor (Figure 3) containing the NIR fluorescent BP NPs increases with time while the fluorescent intensity of the NIR fluorescent control NPs were significantly lower and of the same intensity level at all time periods. This behavior indicates the high specificity of the BP NPs to the osteosarcoma tumor, due to the increase in Ca^{+2} concentration in the Saos-2 tumor environment [42,43], causing an increased uptake of the BP NPs.

After establishing the tumor targeting ability of the BP NPs, the therapeutic ability of the free doxorubicin doxorubicin-conjugated BP NPs were examined. Before testing on the CAM model, cell toxicity was evaluated on osteosarcoma cells. For this purpose, we compared the activity of 50 and 250 ng/ml free doxorubicin and the same concentration of doxorubicin conjugated to the BP NPs on Saos-2 and U-2OS cell lines. Figure 4 summarizes the results of these trials. This figure first of all exhibits that the non- conjugated BP NPs do not possess any toxicity to both cell lines. In addition, this figure illustrates that the % cell viability of the Saos-2 cell line treated with free doxorubicin is significantly higher than that of the doxorubicin-conjugated BP NPs. The treatment with 50 ng/ml non-conjugated or conjugated doxorubicin over 48 h exhibits 77 and 46 % cell viability, respectively, and a further decrease in the cell viability was shown after 72 h, 53 and 35 %, respectively. When treated with a concentration 250 ng/ml doxorubicin a more dramatic difference between the free doxorubicin to the doxorubicin-conjugated BP NPs was illustrated. Treatment for 48 h showed 58 and 10 % viability, respectively, and for 72h 44 and 11 %, respectively. A similar effect was noticeable when U-2OS cells were treated with free doxorubicin and doxorubicin-conjugated BP NPs. For treatment of 50 ng/ml over 48 h the cell viability was 89% compared to 26%, respectively and for 72 h 74 and 21 % viability, respectively. A slight smaller difference was noticeable when treated with 250 ng/ml doxorubicin, over 48h was 40 and 23 % viability, and over 72 h was 30 and 22 % viability, respectively.

To summarize, these findings show that the doxorubicin-conjugated BP NPs were significantly more potent and toxic than the free doxorubicin in both types of osteosarcoma cells. In contrast, the BP NPs as control, do not exhibit any toxicity to these cells.

Further studies on the uptake of the BP NPs were performed, by initially conjugating the fluorescent dye Cy3 to the free amine of the BP NPs (as described in the experimental part), to enable the use of a fluorescent and confocal microscopy with a filter of ex 3ex 512 3em 570 nm. For this purpose U-2OS cells were incubated for 1, 4 and 24 h with the Cy3-conjugated BP NPs (0.16 mg/ml). Cell uptake was analyzed using fluorescence microscope (Zeiss, Axio imager Z1). The images (Figure 5) clearly show that after 1 h the Cy3-conjugated BP NPs penetrate the cells, and after 24 h the Cy3-conjugated BP NPs are more concentrated in the cytoplasm, as seen in Figure 5C. The cell uptake to the cytoplasm was confirmed by confocal microscope. The experiment cannot repeat with the doxorubicin-conjugated BP NPs due to cell apoptosis, however we hypothesize that doxorubicin-conjugated BP NPs will also penetrate the cell. The doxorubicin will then be cleaved

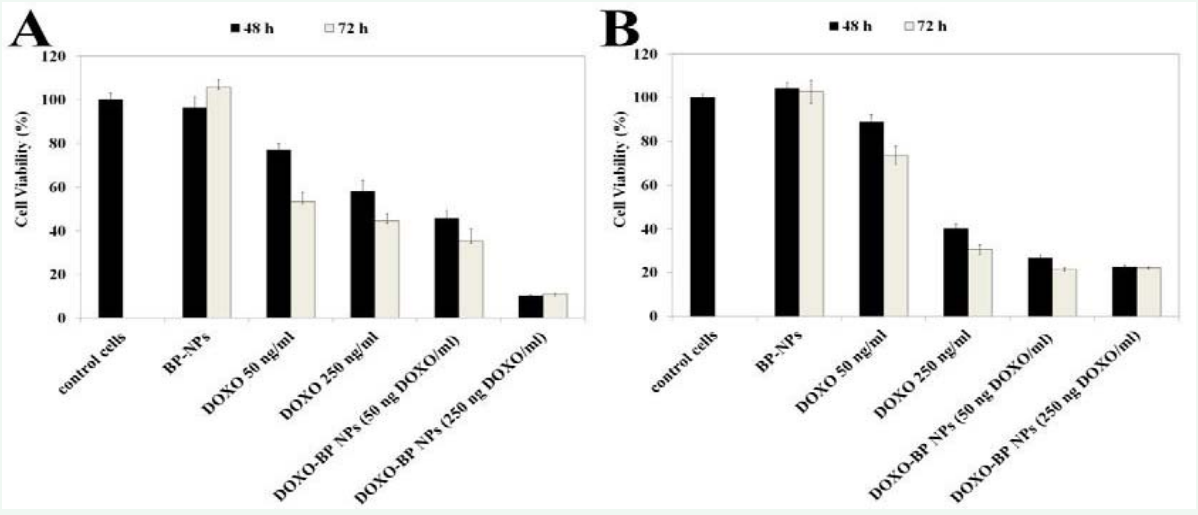

Figure 4 Doxorubicin and doxorubicin-conjugated BP NP (doxo-BP) toxicity in Saos-2, (A) and U-2OS (B) cell lines. Cells were treated for 48 and 72 h with 50 or 250 ng/ml free doxorubicin (doxo) or with equivalent concentration of doxorubicin conjugated to the BP NPs. (Error bars represent standard deviation).

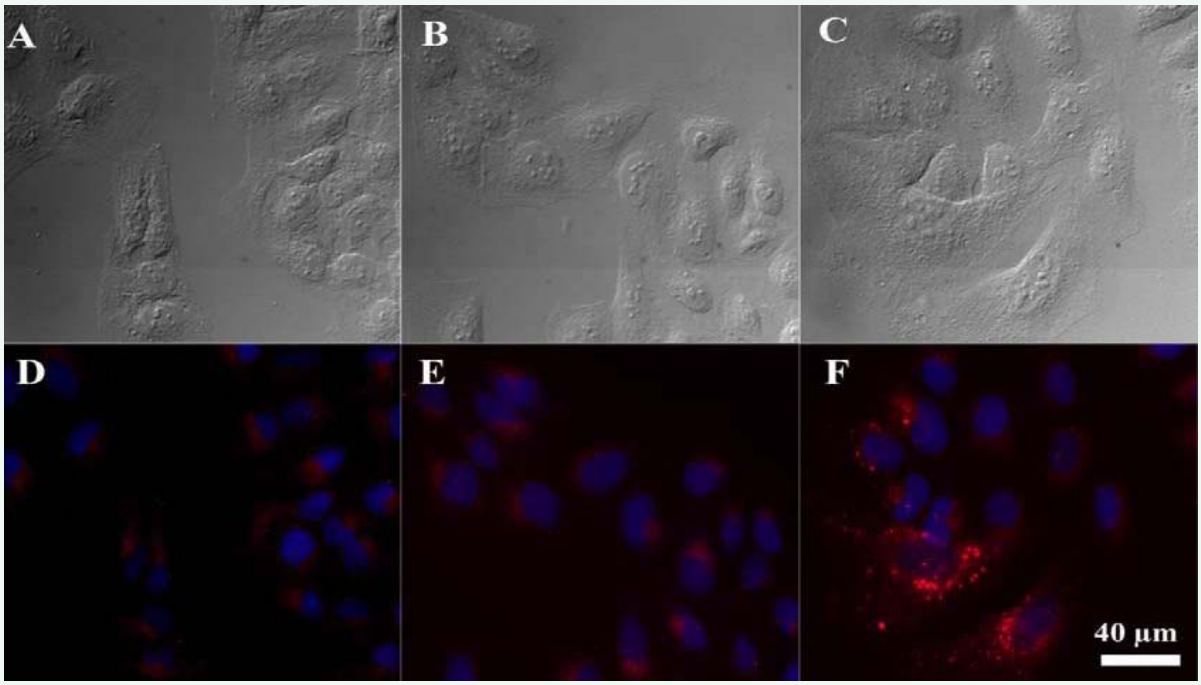

Figure 5 Uptake of Cy3-conjugated BP NPs in U-2OS cells. U-2OS cells were incubated for 1 (A, D), 4 (B, E) and 24 (C, F) h with Cy3 conjugated BP NPs (0.16 mg/ml) Images were taken in bright field (A-C) and merged fluorescent images (D-F) red represents Cy3-conjugated BP NPs and nucleus is seen in blue (hocsht).

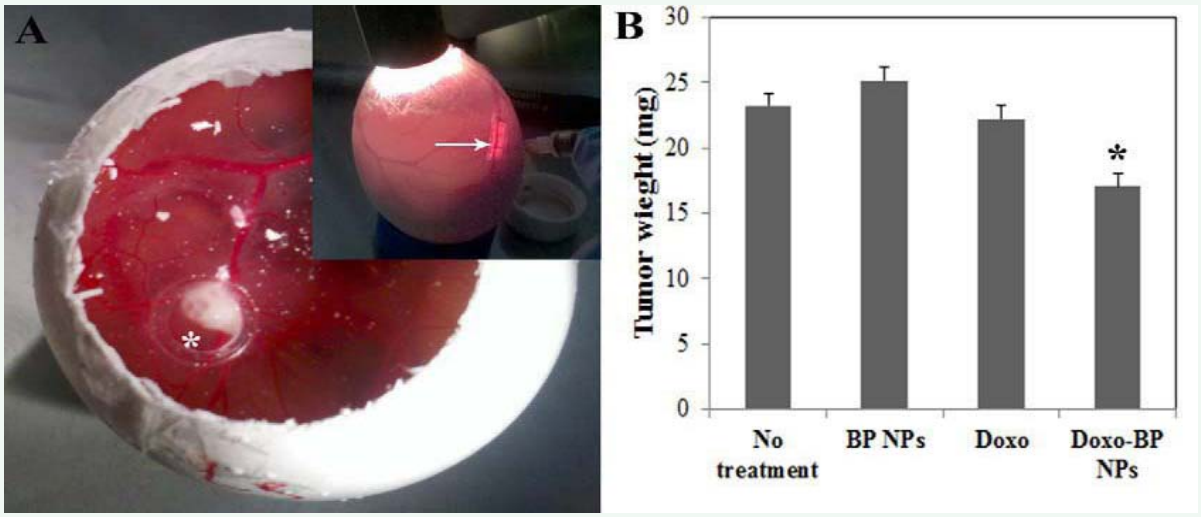

Figure 6 The CAM tumor assay: topical view of the tumor and IV administration of NPs (A) and the therapeutic activity of the doxorubicin-conjugated BP NPs in a CAM model (B). On E8 of incubation, a window was opened in the eggs' shell, and the CAM was exposed. A total of 6 x 105 Saos-2 cells were implanted in a plastic ring placed on the CAM (*). On E13, a total of 100 µL PBS containing 0.1 mg/mL of BP NPs or 0.1 mg/ml doxorubicin-conjugated BP NPs (0.5 µg doxo/ml or 10 µg/ml free doxorubicin were IV injected (as pointed out by the arrow). (B) After 96 h the doxorubicin-conjugated BP NPs have prevented the tumor growth significantly ($p < 0.05$), contrarerily to the BP NPs and free doxorubicin which did not show any therapeutic effect. (Error bars represent standard error).

in the cytoplasm by enzymes allowing the free doxorubicin to reach the DNA and inhibit the enzyme topoisomerase II thus preventing DNA replication [44].

The therapeutic activity of the doxorubicin conjugated to the BP NPs was further investigated using the CAM model. Experiments were carried out similar to those described for the targeting ability of the BP NPs (paragraph 2.8). 0.1 mg/ml BP NPs, 0.1 mg/ml doxorubicin-conjugated BP NPs (0.5 µg doxo/ml) and free doxorubicin (10 µg/ml**)** dispersed/dissolved in PBS were injected IV into the chicken embryos and the tumor was excised and weighed after 96 h. Figure 6 indicates that even though the concentration of the conjugated doxorubicin was 20 times less than that of the free doxorubicin (0.5 and 10 µg, respectively) it

prevented the tumor growth significantly ($p < 0.05$). On the other hand, no significant differences were noted between BP NPs, free doxorubicin and untreated tumors. Hence we can conclude that the doxorubicin-conjugated BP NPs have a high affinity to osteosarcoma tumors attributed to the presence of the BP groups in comparison to the free doxorubicin which probably dispersed unselectively all over the chicken embryos body. The greater therapeutic effect of the doxorubicin-conjugated BP NPs is due to the polyvalency effect, which is a cause of a high concentration delivered to the tumor by the NPs. This confirms results shown in earlier studies that suggest that nanoparticle drug delivery improves both the uptake and therapeutic response of anticancer drugs by tumors [45].

SUMMARY AND CONCLUSION

In this study, we engineered a new doxorubicin-conjugated BP NPs for the treatment of osteosarcoma. These doxorubicin-conjugated BP NPs may prove to be very useful for the *in vivo* treatment of bone tumors, due to their high affinity to Ca^{+2}, allowing the delivery of high concentrations of doxorubicin directly to the tumor and thus reducing the side effects. We have demonstrated that conjugation of doxorubicin to BP NPs significantly increases the anti-cancer activity of the drug against osteosarcoma cell lines in comparison to the free drug. This was further investigated in a CAM model were we verified the affinity and the therapeutic activity of the doxorubicin-conjugated BP NPs to osteosarcoma tumors. The results obtained showed that the targeted delivery of doxorubicin significantly increased the efficacy of the anti-cancer drug, thus allowing the efficient use of low concentration of doxorubicin.

In future work, we plan to extend this study to *in vivo* mouse models, allowing us to study the body distribution and t1/2 of the BP NPs, as well as confirming the targeting and therapeutic activity of the doxorubicin-conjugated BP NPs. Moreover, by conjugating other suitable drugs, these BP NPs may be used for treatment of other bone diseases where there is a high rate of bone resorption.

ACKNOWLEDGMENT

This study was supported by the Israeli Ministry of Commerce and Industry (Kamin Grant). The authors thank Dr. Ronen Yehuda for his assistance with the fluorescent images. The authors also thank Mr. Hai Haham for his assistance with the TEM images.

REFERENCES

1. Picci P. "Classic Osteosarcoma"; In Atlas of Musculoskeletal Tumors and Tumorlike Lesions; Springer International Publishing, 2014; 1: 147-152.
2. Hauben EI, Arends J, Vandenbroucke JP, van Asperen CJ, Van Marck E, Hogendoorn PC. Multiple primary malignancies in osteosarcoma patients. Incidence and predictive value of osteosarcoma subtype for cancer syndromes related with osteosarcoma. Eur J Hum Genet. 2003; 11: 611-618.
3. Ferguson WS, Goorin AM. Current treatment of osteosarcoma. Cancer Invest. 2001; 19: 292-315.
4. Bacci G, Picci P, Ruggieri P, Mercuri M, Avella M, Capanna R, et al. Primary chemotherapy and delayed surgery (neoadjuvant chemotherapy) for osteosarcoma of the extremities. The Istituto Rizzoli Experience in 127 patients treated preoperatively with intravenous methotrexate (high versus moderate doses) and intraarterial cisplatin. Cancer. 1990; 65: 2539-2553.
5. Saeter G, Alvegård TA, Elomaa I, Stenwig AE, Holmström T, Solheim OP. Treatment of osteosarcoma of the extremities with the T-10 protocol, with emphasis on the effects of preoperative chemotherapy with single-agent high-dose methotrexate: a Scandinavian Sarcoma Group study. J Clin Oncol. 1991; 9: 1766-1775.
6. Benassi MS, Chiechi A, Ponticelli F, Pazzaglia L, Gamberi G, Zanella L, et al. Growth inhibition and sensitization to cisplatin by zoledronic acid in osteosarcoma cells. Cancer Lett. 2007; 250: 194-205.
7. Roche B, Vanden-Bossche A, Normand M, Malaval L, Vico L, Lafage-Proust M-H. "Validated Laser Doppler protocol for measurement of mouse bone blood perfusion— Response to age or ovariectomy differs with genetic background. Bone. 2013; 55: 418- 426.
8. Paulussen M, Ahrens S, Lehnert M, Taeger D, Hense HW, Wagner A, et al. Second malignancies after ewing tumor treatment in 690 patients from a cooperative German/Austrian/Dutch study. Ann Oncol. 2001; 12: 1619-1630.
9. Bacci G, Ferrari S, Mercuri M, Longhi A, Capanna R, Tienghi A, et al. Neoadjuvant chemotherapy for extremity osteosarcoma--preliminary results of the Rizzoli's 4th study. Acta Oncol. 1998; 37: 41-48.
10. Reid IR, Hosking DJ. Bisphosphonates in Paget's disease. Bone. 2011; 49: 89-94.
11. Clézardin P, Benzaïd I, Croucher PI. Bisphosphonates in preclinical bone oncology. Bone. 2011; 49: 66-70.
12. Miller PD. The kidney and bisphosphonates. Bone. 2011; 49: 77-81.
13. Eastell R, Walsh JS, Watts NB, Siris E. Bisphosphonates for postmenopausal osteoporosis. Bone. 2011; 49: 82-88.
14. Owens G, Jackson R, Lewiecki EM. An integrated approach: bisphosphonate management for the treatment of osteoporosis. Am J Manag Care. 2007; 13 Suppl 11: S290-308.
15. Rogers MJ, Crockett JC, Coxon FP, Mönkkönen J. Biochemical and molecular mechanisms of action of bisphosphonates. Bone. 2011; 49: 34-41.
16. Russell RG, Watts NB, Ebetino FH, Rogers MJ. Mechanisms of action of bisphosphonates: similarities and differences and their potential influence on clinical efficacy. Osteoporos Int. 2008; 19: 733-759.
17. Papapoulos SE. Bisphosphonates: how do they work? Best Pract Res Clin Endocrinol Metab. 2008; 22: 831-847.
18. Rogers MJ, Gordon S, Benford HL, Coxon FP, Luckman SP, Monkkonen J, et al. Cellular and molecular mechanisms of action of bisphosphonates. Cancer. 2000; 88: 2961-2978.
19. Bisaz S, Jung A, Fleisch H. Uptake by bone of pyrophosphate, diphosphonates and their technetium derivatives. Clin Sci Mol Med. 1978; 54: 265-272.
20. Cho K, Wang X, Nie S, Chen ZG, Shin DM. Therapeutic nanoparticles for drug delivery in cancer. Clin Cancer Res. 2008; 14: 1310-1316.
21. An SY, Bui MP, Nam YJ, Han KN, Li CA, Choo J, et al. Preparation of monodisperse and size-controlled poly(ethylene glycol) hydrogel nanoparticles using liposome templates. J Colloid Interface Sci. 2009; 331: 98-103.
22. Kim K, Lee M, Park H, Kim JH, Kim S, Chung H, et al. Cell-permeable and biocompatible polymeric nanoparticles for apoptosis imaging. J Am Chem Soc. 2006; 128: 3490-3491.
23. Masarachia P, Weinreb M, Balena R, Rodan GA. Comparison of the

distribution of 3H-alendronate and 3H-etidronate in rat and mouse bones. Bone. 1996; 19: 281-290.

24. Corem-Salkmon E, Ram Z, Daniels D, Perlstein B, Last D, Salomon S, et al. Convection-enhanced delivery of methotrexate-loaded maghemite nanoparticles. Int J Nanomedicine. 2011; 6: 1595-1602.

25. Hamidi M, Azadi A, Rafiei P. Hydrogel nanoparticles in drug delivery. Adv Drug Deliv Rev. 2008; 60: 1638-1649.

26. Yang SR, Lee HJ, Kim JD. Histidine-conjugated poly(amino acid) derivatives for the novel endosomolytic delivery carrier of doxorubicin. J Control Release. 2006; 114: 60-68.

27. Cohen S, Pellach M, Kam Y, Grinberg I, Corem-Salkmon E, et al. Synthesis and characterization of near IR fluorescent albumin nanoparticles for optical detection of colon cancer. Mater Sci Eng C. 2013; 33: 923-931.

28. Maeda H. The enhanced permeability and retention (EPR) effect in tumor vasculature: the key role of tumor-selective macromolecular drug targeting. Adv Enzyme Regul. 2001; 41: 189-207.

29. Allen TM. Ligand-targeted therapeutics in anticancer therapy. Nat Rev Cancer. 2002; 2: 750-763.

30. Babu A, Templeton AK, Munshi A, Ramesh R. Nanodrug delivery systems: a promising technology for detection, diagnosis, and treatment of cancer. AAPS PharmSciTech. 2014; 15: 709-721.

31. Gluz E, Grinberg I, Corem-Salkmon E, Mizrahi D, Margel S. Engineering of new crosslinked near-infrared fluorescent polyethylene glycol bisphosphonate nanoparticles for bone targeting. J Polym Sci A Polym Chem. 2013; 51: 4282-4291.

32. Gluz E, Mizrahi DM, Margel S. Synthesis and characterization of new poly (ethylene glycol) bisphosphonate vinylic monomer and non-fluorescent and NIR-fluorescent bisphosphonate micrometer-sized particles. Polymer. 2013; 54: 565-571.

33. Mizrahi DM, Ziv-Polat O, Perlstein B, Gluz E, Margel S. Synthesis, fluorescence and biodistribution of a bone-targeted near-infrared conjugate. Eur J Med Chem. 2011; 46: 5175-5183.

34. Gluz E, Rudnick-Glick S, Mizrahi DM, Chen R, Margel S. New biodegradable bisphosphonate vinylic monomers and near infrared fluorescent nanoparticles for biomedical applications. Polymer Adv Tech. 2014; 25: 499-506.

35. Veronese FM, Mero A. The impact of PEGylation on biological therapies. BioDrugs. 2008; 22: 315-329.

36. Grinberg I, Dukhovny A, Goldstein RS. A rapid and simple assay for human blood malignancy engraftment, homing and chemotherapy treatment using fluorescent imaging of avian embryos. Leuk Lymphoma. 2012; 53: 472-478.

37. Dufrane D, Delloye C, McKay IJ, De Aza PN, De Aza S, Schneider YJ, et al. Indirect cytotoxicity evaluation of pseudowollastonite. J Mater Sci Mater Med. 2003; 14: 33-38.

38. Budini M, Buratti E, Stuani C, Guarnaccia C, Romano V, De Conti L, et al. Cellular model of TAR DNA-binding protein 43 (TDP-43) aggregation based on its C-terminal Gln/Asn-rich region. J Biol Chem. 2012; 287: 7512-7525.

39. Shibata K, Kudo Y, Tsunoda M, Hosokawa M, Sakai Y, Kotani M, et al. Magnetometric evaluation of the effects of man-made mineral fibers on the function of macrophages using the macrophage cell line RAW 264.7. Ind Health. 2007; 45: 426-436.

40. Grinberg I, Reis A, Ohana A, Taizi M, Cipok M, Tavor S, et al. Engraftment of human blood malignancies to the turkey embryo: a robust new in vivo model. Leuk Res. 2009; 33: 1417-1426.

41. Noiman T, Buzhor E, Metsuyanim S, Harari-Steinberg O, Morgenshtern C, Dekel B, et al. A rapid in vivo assay system for analyzing the organogenetic capacity of human kidney cells. Organogenesis. 2011; 7: 140-144.

42. Yamaguchi T, Kifor O, Chattopadhyay N, Brown EM. Expression of extracellular calcium (Ca2 + o)-sensing receptor in the clonal osteoblast-like cell lines, UMR-106 and SAOS-2. Biochem Biophys Res Commun. 1998; 243: 753-757.

43. Lemomt UG, Strong DD, Mohan S, Demarest K, Baylink DJ. Effect of progesterone on the mRNA levels of insulin-like-growth factors (IGFs), IGF-binding proteins (JGFBPs) and type-1 and -type-2 igfreceptors in human osteoblastic cells. Bone and Mineral. 1992; 17: 86.

44. Fornari FA, Randolph JK, Yalowich JC, Ritke MK, Gewirtz DA. Interference by doxorubicin with DNA unwinding in MCF-7 breast tumor cells. Mol Pharmacol. 1994; 45: 649-656.

45. Kukowska-Latallo JF, Candido KA, Cao Z, Nigavekar SS, Majoros IJ, Thomas TP, et al. Nanoparticle targeting of anticancer drug improves therapeutic response in animal model of human epithelial cancer. Cancer Res. 2005; 65: 5317-5324.

Cite this article

Rudnick-Glick S, Corem-Salkmon E, Grinberg I, Gluz E Margel S (2014) Doxorubicin-Conjugated Bisphosphonate Nanoparticles for the Therapy of Osteosarcoma. JSM Nanotechnol Nanomed 2(2): 1022.